Bifacial and Monofacial PV Systems Performance Assessment Based on IEC 61724-1 Standard

Emanuele Ogliari, *Member, IEEE*, Alberto Dolara, *Member, IEEE*, Domenico Mazzeo, *Member, IEEE*, Giamplaolo Manzolini, and Sonia Leva, *Senior Member, IEEE*

***Abstract*—The performance of bifacial photovoltaic (bPV) modules under various operating conditions needs to be analyzed with research and development activities. This research work performed an experimental comparison of the energy performance of a bPV module and a monofacial photovoltaic (mPV) module, based on experimental data measured at SolarTech^{LAB}, Department of Energy, Politecnico di Milano. For this purpose, the performance ratio (PR) and the temperature-corrected PR proposed by the IEC 61724-1 standard for bPV and mPV modules were evaluated. To calculate the energy improvement of the technology in terms of bifacial gain, measurements were recorded during the period from 8 June to 31 November, 2022, of PV modules facing south, ground-mounted and with a low albedo. It was found that the PR relative gain of the bPV compared with the mPV module is 10.8% higher in the whole period. Moreover, the presence of a commercial white plastic sheet with high reflectivity located beneath the bPV modules from 28 May to 5 June, 2022, showed an additional increase in the bPV PR of 0.0165, corresponding to a relative difference increased by 20%.**

***Index Terms*—Bifacial photovoltaic (bPV), performance ratio (PR), photovoltaic (PV).**

I. Introduction

ACCORDING to a study conducted by the International Energy Agency, photovoltaic (PV) systems accounted for only 3.7% of the electricity demand in the world in 2020 [1] and the bifacial PV (bPV) cell technology market share is expected to reach nearly 30% by 2028 [2]. bPV modules capture the sunlight from both sides of the module and, therefore, compared with the traditional monofacial PV (mPV) modules, between 6% and 10% [3]. Bifacial gain, defined as the ratio between the output power of a bPV module and the output power of an equivalent module with the front-side only, is commonly used to make this comparison [4].

By examining [5] and [6], the following can be concluded:

i) bPV modules typically run cooler than monofacial;
ii) when rear irradiance is especially high, the bPV module may run hotter;
iii) even so, the energy gain from bPV module response outweighs the energy loss from higher temperature.

The study conducted by Liu et al. [6] quantified that the difference in nominal module operating temperature (NMOT) between a bPV and mPV, according to the IEC 61853-2:2016 [7], is around an average value of $-1.1\,^{\circ}$C, in the face of a difference between the rated NMOT of $-1\,^{\circ}$C.

The performance of bPV modules with fixed structures is primarily function of the ground albedo, the elevation of the module above the ground, as well as the module inclination and orientation, namely its tilt and azimuth angles [8].

Owing to its higher albedo, an aluminium surface placed on the ground leads to a higher energy production of a bPV module compared with a grass surface [9]. Moreover, another study demonstrated that for a day with snow on the ground, the specific daily yield for the bPV module increased by 12% although the daily irradiation in the plane was lower in the snowy day [10].

Another important variable is the height of the bPV module from the ground, which also influences the energy yield because the rear irradiance is being modified [11]. At low height, the backside irradiance is significantly reduced due to self-shadowing [12]. The backside of the module gets more irradiation of the sky and the ground reflected radiation increases with the height from the ground. However, there is a saturation effect at which the effect of elevation becomes less relevant [13].

The tilt angle significantly influences the performance of bPV modules. The optimal tilt angle of the bPV module for a given location is higher compared with the mPV ones [9], [14]. In addition, the backside irradiance is less affected by the tilt angle than the front-side one [1]. Finally, it was investigated that the height, albedo, system size, and time of the year are relevant parameters to estimate the optimal value of the tilt angle [12], [13].

Another parameter that significantly affects the bPV energy yield is the module orientation. A recent experimental research detected that the highest average power output for the northern hemisphere is reached when the panel is facing to the southern orientation [9]. However, the variation with the other orientations is limited, meaning that bPV technology is more flexible compared to the mPV.

From the analysis of the literature, capacity testing and energy comparisons of bPV and mPV modules are the most common approach used to quantify the enhanced performance of bPV

Manuscript received 20 January 2023; revised 12 April 2023 and 15 June 2023; accepted 8 July 2023. Date of publication 31 July 2023; date of current version 6 September 2023. This work was supported by the Agritech National Research Center, European Union Next-GenerationEU (PIANO NAZIONALE DI RIPRESA E RESILIENZA (PNRR)—MISSIONE 4 COMPONENTE 2, INVESTIMENTO 1.4) under Grant D.D. 1032 17/06/2022 and Grant CN00000022. *(Corresponding author: Emanuele Ogliari.)*

The authors are with the Department of Energy, Politecnico di Milano, 20133 Milano, Italy (e-mail: emanuelegiovanni.ogliari@polimi.it; alberto.dolara@polimi.it; domenico.mazzeo@polimi.it; giampaolo.manzolini@polimi.it; sonia.leva@polimi.it).

Color versions of one or more figures in this article are available at https://doi.org/10.1109/JPHOTOV.2023.3295869.

Digital Object Identifier 10.1109/JPHOTOV.2023.3295869

modules. Capacity tests are widely used during the contracting and acceptance testing of PV systems. With the increasing deployment of bPV modules, there is a need to develop a standardized approach to capacity test these systems. Although variability and bias error were inherently higher for the measured capacity of bPV systems, they could be reduced to a level consistent with the mPV reference system by appropriate incorporation of rear irradiance either measured or modeled. Capacity tests as ASTME2848-13 [15] and IEC TS 61724-2 [16] are adopted to assess the PV system performance under actual environmental conditions. According to ASTM 2848-13 regression method, ac power is correlated with plane-of-array irradiation, ambient temperature, and wind speed. In this context, some researchers proposed some modifications and applied the aforementioned methodology to develop a standardized approach also for bPV modules [17], [18]. Several studies were carried out in recent years to compare the energy performance of mPV and bPV modules. For example, a bifacial gain of 19% during winter was found in the snowy environment of Escanaba, Michigan [19], while changing the rear encapsulation material from white to a transparent encapsulation improved the bifaciality to 15.1% compared with the reference 3.46% on a carport system in the southwestern part of the Korean Peninsula [20].

Considering the wide range of energy gain values and the variety of cases presented in the literature, there is no clear indication of the energy yield comparison between bPV and traditional mPV. Therefore, research should focus on experimental campaigns for accumulating data in situ to clarify the impact of different design parameters on bPV performance, directly comparing them to other PV modules.

This study contributes by comparing the normalized energy performance indexes proposed by the IEC 61724-1 standard of a bPV system with those of an mPV system. On-field measurements of both bPV and mPV modules were performed at SolarTech^{LAB} [21] of Politecnico di Milano, Italy.

As a special case, the work also aims to analyze the impact of a commercial white plastic sheet with high reflectivity located beneath the bPV module. Solar irradiance, temperature, and ac power were measured for each configuration and a fixed tilt angle of 30° to assess the performance of the arrays under the same environmental conditions over a period of nearly six months.

The rest of this article is organized as follows. The adopted methodology and the reference standards are described in Section II. Experimental setup and case study are described in Section III. The experimental results are presented in Section IV in addition to an extended discussion on the results. Finally, Section V concludes this article.

II. Methodology for PV Energy Assessment According to Current Regulation

A. Standard Requirements for PV Energy Assessment

This study presents the analysis of bPV performance according to the IEC 61724-1 standard [22] developed by the International Electrotechnical Commission (IEC). This standard, which was published in 1998, provided guidelines for the measurement of the parameters, monitoring system and performance indices of PV plants. Now, it is currently withdrawn, and it has been partially replaced by introducing monitoring recommendation and performance assessment of bPV systems, and with updates in the requirements on the irradiance sensor, the soiling measurement based on new technology and explanatory notes are added.

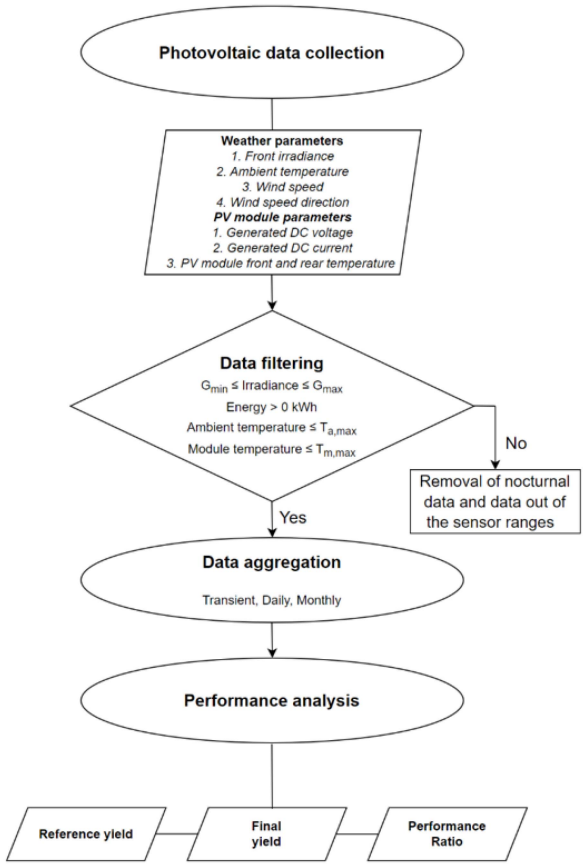

Fig. 1. Flowchart resembling the measurement procedure to assess different PV systems energy performance according to the IEC standards.

IEC 61724-1 contains requirements for system performance monitoring, including equipment characteristics, data sampling and filtering, measured and calculated parameters, and performance metrics. As shown in the flowchart of Fig. 1, the study is based on the collection and analysis of the measurements of climatic factors, which defines the procedure for measuring and analyzing the power generation of a PV system, with two days of minimum duration.

To analyze the performance of the mPV and bPV modules, the same outdoor conditions must take place for each PV module while simultaneously and continuously electrical and climate parameters are recorded. Measurement data acquisition system records PV module output dc voltage and current, module temperature, ambient temperature, air humidity, wind speed, and solar irradiance. The IEC standard also suggests implementing filtering algorithms to detect and eliminate or replace (when possible) erroneous data, as follows:

- not-consistent values originating from failures in the measurement system;

- abrupt changes both in power and irradiance values. Such sudden variations may be associated with rapid changes in irradiance, commonly under partially cloudy skies.

Finally, the standards suggest detecting and reviewing "dead values," i.e., consecutive measurements with identical values. Given that continuous measurement values should generally change, the opposite may indicate faulty data transmission or recording. Therefore, acquired data were filtered to ensure that they are within nominal sensor ranges, using thresholds according to [22].

B. Adopted Methodology for PV Energy Assessment

As shown in Fig. 1, the adopted PV energy assessment methodology, compliant with the abovementioned standards, includes a three-step procedure with data filtering and preparation process, before handling and calculations. First, the recording system from inverters considers the Universal Time Coordinated instead of the local time; thus, a displacement of +1 h for Italian time zone was applied. Second, solar irradiance from the weather station was filtered considering a minimum of 5 W/m^2 to avoid the night period of nonproduction. Specifically, data that met the following criteria were analyzed:

1) 5 $\mathrm{W/m^2} \leq$ Solar irradiance $\leq$ 1,200 $\mathrm{W/m^2}$;
2) Energy $>$ 0 kWh;
3) ambient temperature $\leq$ 50°C;
4) PV module temperature $\leq$ 90 °C.

Finally, as the third step of the procedure, all the data from the different inverters and the weather station were resampled every 5 min to synchronize the different variables and configurations.

C. Performance Indexes

To compare the performance of the different PV configurations, the abovementioned standard [22] provides general guidelines for the analysis of the electrical performance of PV systems of different sizes, operating in different climates, and providing energy for different applications. Normalized indexes, previously defined and adopted in similar research works [23], [24], are calculated for each day of measurement, however they could be calculated on different target time horizons such as: day, weeks, months, and years. The final yield Y_F is defined as

$$Y_F = \frac{E_{\mathrm{out}}}{P_0} \quad (h). \tag{1}$$

It represents the number of hours that the array would need to operate at its rated output power P_0 to equal its monitored contribution to the net energy output load over the target time horizon. E_{out} is the net daily ac energy output of the entire PV installation. Besides, the reference yield Y_R is defined as

$$Y_R = \frac{H_I}{G_{\mathrm{stc}}} \quad (h). \tag{2}$$

It represents the number of the solar irradiance hours which would need to be at the reference irradiance level to contribute the same incident energy as monitored. H_I is the global irradiation on the plane of the array recorded over the target time horizons, and G_{stc} is the solar irradiance of the standard test conditions (STC) that equals 1000 $\mathrm{W/m^2}$.

The bifacial irradiance factor (BIF) is introduced in the standard to correct the measured irradiance terms [22] and to calculate the "effective" irradiance that can be converted by a bifacial device from both the front and rear sides collectively. This factor is dimensionless and multiplies the front-side in-plane irradiance (G_i), or plane-of-array (POA) irradiance, both expressed in units $\mathrm{W/m^2}$. BIF_k refers to the k th sample of time and it has the following expression:

$$\mathrm{BIF}_k = 1 + \phi_{P\max} \cdot \rho_k \tag{3}$$

where

1) $\phi_{P\max}$ is the bifaciality coefficient. It is the ratio between the maximum power of the rear side and the front side of a bifacial device, typically at STC unless, otherwise specified, when the other side is not irradiated; in the presented case, it is provided by the manufacturer;
2) ρ_k is the in-plane rear side irradiance ratio, and it is the ratio of the irradiance incident on the rear side of the modules in the PV array to the irradiance incident on the front side.

Therefore, for bPV, the following equations for the reference yield Y_R^{bi} has to be considered:

$$Y_R^{\mathrm{bi}} = \frac{\sum_k (G_{i,k} \cdot \tau_k \cdot \mathrm{BIF}_k)}{G_{\mathrm{stc}}} \quad (h) \tag{4}$$

where $G_{i,k}$ is the in-plane irradiance kth sample, τ_k is the sampling time, and the sum of the samples is extended over the recorded target time horizons. Finally, the performance ratio (PR) of an mPV system is defined as the ratio between Y_F and Y_R for the period of measurement

$$\mathrm{PR} = \frac{Y_F}{Y_R}. \tag{5}$$

It is a dimensionless quantity that indicates the amount of the net output energy of the PV system, compared with the theoretical one in input for a certain period. It represents the overall effect of the component's efficiency in the actual operating conditions.

The seasonal variation of the performance ratio PR reported in (5), which is also affected by other factors as seasonally dependent shading or spectral effects, can be significantly reduced by calculating a temperature-corrected performance ratio PR′. The "25 °C performance ratio" ($\mathrm{PR}'_{25^\circ\mathrm{C}}$) is calculated by adjusting the power rating at each recording interval to compensate for differences between the actual PV module temperature and the STC reference temperature of 25 °C. Therefore, the $\mathrm{PR}'_{25^\circ\mathrm{C}}$ formula is

$$\mathrm{PR}'_{25^\circ\mathrm{C}} = \frac{\sum_k (P_{\mathrm{out},k} \cdot \tau_k)}{\sum_k \left(\frac{C_{k,25^\circ\mathrm{C}} \cdot P_0 \cdot G_{i,k} \cdot \tau_k}{G_{\mathrm{stc}}} \right)}. \tag{6}$$

As regards to $C_{k,25^\circ\mathrm{C}}$ coefficient, it is calculated as

$$C_{k,25^\circ\mathrm{C}} = 1 + \gamma \cdot (T_{\mathrm{mod},k} - 25^\circ) \tag{7}$$

where γ is the relative maximum-power thermal coefficient and $T_{\mathrm{mod},k}$ is the kth sample module temperature.

The monofacial performance ratio formulas presented previously, in (5) and (6), can be transformed to the correspondent bifacial performance ratio ones by introducing the aforementioned BIF to correct the measured irradiance terms. Then, even

if their formulas are not explicitly reported in the standard [22], both the performance ratio PR_{bi} and the 25 °C performance ratio ($PR'_{25°C,bi}$) for bPV are here calculated symmetrically as

$$PR_{bi} = \frac{Y_F}{Y_R^{bi}} \tag{8}$$

$$PR'_{25°C,bi} = \frac{\sum_k (P_{out,k} \cdot \tau_k)}{\sum_k \left(\frac{C_{k,25°C} \cdot P_0 \cdot G_{i,k} \cdot BIF_k \cdot \tau_k}{G_{stc}} \right)} \tag{9}$$

where $P_{out,k}$ is the kth ac power output sample.

III. Case Study

The experimental activities were carried out at the laboratory SolarTech^{LAB} [21], Politecnico di Milano, Italy, with geographical coordinates of latitude 45°30′10.588″N and longitude 9°9′23.677″E, in the period from 28 May to 20 November, 2022. A recent study carried out in the Milan climate, which is characterized by relatively cold winters and warm summers, has shown that the reduction in annual PV energy production observed due to climate change will be less significant in the future, both in low and high greenhouse gas emission scenarios [25]. As the main purpose of these tests was to assess the increase in the energy production of bPV technology in contrast to traditional mPV technology, in the same environmental conditions. Furthermore, the effect of ground reflectivity on bPV energy production was experimentally evaluated by means of a specific test campaign.

The experimental setup consists of two grid-connected PV systems based on bPV and mPV modules, respectively. Each PV system consists of a PV string and an inverter, the latter operates the PV generator at its maximum power point (MPP). From the electrical point of view, the operation of the bPV generator is independent of the operation of mPV generator, and vice versa. The details of the systems are as follows:

1) bPV system consists of a string of two bPV modules in series with glass–glass cover (Enel Green Power 3SBA345 A) connected to a Solis inverter (Type S6-GR0.7PK-M). The installed power of the bPV generator is 690 W;
2) mPV system consists of a string of four mPV modules in series (ALEO Solar S59-305) connected to a Solis inverter (Type S6-GR1P1K-M). The installed power of mPV generator is 1, 220 W.

Since the final yield also depends on the system rating, and the actual maximum power of each PV module could be different from the rated maximum power because of power tolerance and ageing, the $I - V$ curves of the PV modules involved in the test campaign were previously measured in STC according to [4] and [26] and to the procedure described in [27]. It was verified that the maximum power in STC is within the range specified by the manufacturer for each PV module; therefore, the PV system rated power has been taken into account for the final yield calculation.

The main ratings of PV modules and inverters making up the two PV systems are summarized in Tables I and II, respectively. According to the datasheet of the Enel Green Power 3SBA345 A bPV module, data are referred to the front-illuminated conditions; in the so-called bifacial standard test conditions (STC), the maximum module power at STC increases from 345 to 385 W. Inverters are from the same manufacturer, belong to the same inverter series, have similar power ratings and the same maximum ed EU efficiencies. The resulting ratios between the PV generators maximum power at STC and the inverters maximum output power are 89.6% and 110.9%, respectively, for the bPV and mPV systems. The oversizing of the mPV string is widely within the maximum dc power recommended by the manufacturer. As a result, the efficiencies of the inverters with the same irradiance on the mPV and bPV generators are very similar, introducing a negligible contribution to the difference between the final yields of the PV systems.

Fig. 2(a) shows the bPV generator, and Fig. 2(b) shows the mPV generator. Both PV generators have the same orientation, that is tilt 30° and azimuth 6°30′ toward the east (assuming 0° as the south direction), and they are installed close to each other within the test facility to be characterized by similar values of radiation and albedo, as it was experimentally verified at the beginning of the test campaign. Concerning the bPV installation, their lower edge is 14 cm from the floor, while the height of their higher edge is 113 cm. Being the test facility located above technical rooms on the roof floor of a building, its floor is a metallic grid (see Fig. 2) and its albedo was found to be 0.09.

In the period from 28 May, 2022, to 5 June, 2022, a commercial white plastic sheet was placed on the metallic grid under the bPV modules to simulate a high albedo situation, similar to the one that characterizes the ground covered by snow. In this case, it was experimentally verified that albedo that characterizes the rear side of the bPV modules is 0.32. This configuration

TABLE I
Typical Performances at STC and General Characteristics of bPV and mPV Modules

PV module technical feature	bPV	mPV
Model	Enel 3SBA345A	Aleo S59_305
Maximum power (W)	345	305
Maximum array power (W)	690	1220
Maximum power voltage (V)	39.3	31.4
Maximum power current (A)	8.78	9.72
Open circuit voltage (V)	47.90	39.60
Short-circuit current (A)	9.18	10.06
Efficiency (%)	17.40	18.60
Number of cells in a module	72	60
Cell dimensions (mm × mm)	156.75 × 156.75	156.75 × 156.75
Cell technology	Monocrystalline	Monocrystalline
Thermal Power coeff. γ (%/°C)	-0.38	-0.40
NOCT (°C)	44	48
Bifaciality Coefficient ϕ_{Pmax} (p.u.)	0.85	n.a.

Electrical values measured under STC: 1,000 W/m^2, 25°C, AM 1.5.

TABLE II
General Characteristics of Solar Inverters

Inverter Specification	Solis (bPV)	Solis (mPV)
Model	S6-GR1P0.7K-M	S6-GR1P1K-M
Recommended max. dc power (W)	1,100	1,500
Max dc voltage (V)	600	600
Max dc input current (A)	14	14
Max dc short circuit current (A)	22	22
MPPT voltage range (V)	50–500	50–500
Rated ac power output (W)	700	1,000
Max ac power output (W)	770	1,100
EU efficiency (%)	95.3	95.3

Fig. 2. PV arrays experimental layout. (a) Two bPV modules. (b) Four mPV modules.

was designed to enhance the effect of albedo on bPV energy generation. After that, the white sheet was removed to configure the experimental setup in a more realistic arrangement. The latter configuration stands from 8 June, 2022, to 20 November, 2022.

The installation site within the test facility was chosen to be free of shadings on the PV generators by nearby objects for most of the day; they are experienced only at sunrise and sunset, and they affect the power output of both PV generators in a very similar way.

In addition to power conversion, the inverters also provide and make available several electrical measurements, such as voltage, current, power, and energy on both the dc and ac sides; these data refer to a 5-min time interval and were transferred to a PC to be stored. It has been verified that the accuracy of the two inverters involved the experimental activities is quite similar. For the calculation of the performance indexes introduced in Section II-C, only the energy generated on the ac side is necessary.

The environmental conditions are monitored with a meteorological station equipped with solar irradiance sensors, temperature and humidity sensors, wind speed and direction sensors, and a rain collector. Solar irradiance sensors are two secondary standard pyranometers that measure the global horizontal irradiance (GHI) and the global tilted irradiance (GTI) on the plane of PV generators, therefore corresponding to the POA irradiance on the front side. In addition, a pyranometer with a shadow band measures the diffuse horizontal irradiance. The meteorological station provides and makes available the whole set of raw data every 10 s. Further details related to the meteorological station can be found in [27]. For the calculation of the performance indexes introduced in Section II-C, GTI is the source of raw data to calculate the radiation on the front side over the target time horizon, while the radiation on the back side has been calculated from the GHI, together with the experimental values of albedo and the tilt angle [28].

IV. Results and Discussion

The raw data obtained during the whole experimental campaign for both the PV systems, mPV and bPV, were processed to get the performance indexes that allows comparing the performances of the two PV technologies. Fig. 3 shows a selection of preprocessed raw data, consisting of the per unit power curves; the base unit is the power capacity of each PV system (i.e., 1,220 W for mPV and 690 W for bPV). The same week was selected for each month of the analyzed period for comparison. Power curves of bPV and mPV are completely similar: this validates the experimental setup design and confirms that both inverters operate the PV generators at their MPP. The comparison among months highlights the seasonal variations of both the path of the sun in the sky and the weather conditions. Per unit power curves demonstrate that the bPV modules' power output is higher than the mPV power output in every operating condition, resulting in a higher final yield, thanks to the additional contribution to power conversion of the bPV module rear side.

TABLE III
Final Yield Comparison

Final yield	mPV	bPV	Relative difference (%)
Daily Mean (h/day)	3.92	4.31	10.05
June* (h/month)	118.17	129.29	9.41
July (h/month)	165.22	181.62	9.93
August (h/month)	149.43	164.39	10.01
September (h/month)	110.87	117.58	6.05
October (h/month)	75.57	86.89	14.98
November** (h/month)	31.39	36.24	15.46
Whole (h/period)	650.65	716.02	10.05

$\star$ From 8^{th} June. $\star\star$ Until 20^{th} November.

Fig. 4 shows the final yield for both PV technologies computed on a daily basis for the whole testing period, highlighting the increase in energy generation proper to bPV technology. The final yields for both PV technologies were also calculated on a monthly basis and for the whole testing period; the latter pair is then divided by the number of days in the testing period and referred to as the "mean daily final yield." Table III summarizes the mean daily final yield and the monthly final yield for each analyzed month.

The relative difference in final yield between mPV and bPV characterizing autumn months is higher than the same relative difference characterizing summer months. These results are mainly due to the availability of the primary energy source, and the solar irradiance components. The summer months consist of

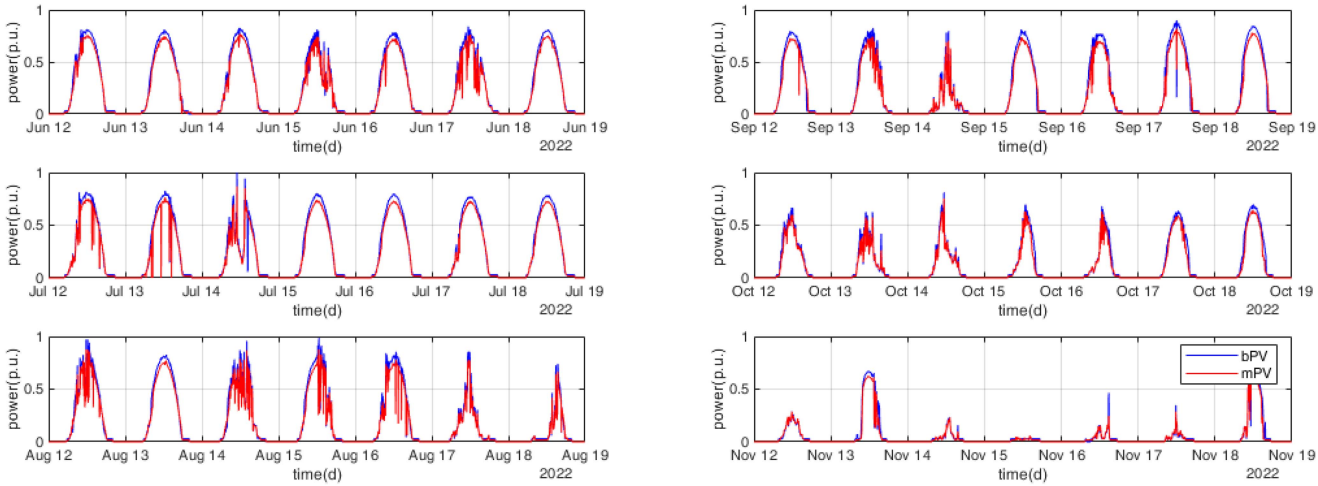

Fig. 3. Comparison of the power production for the analyzed months of the mPV (red) and bPV (blue).

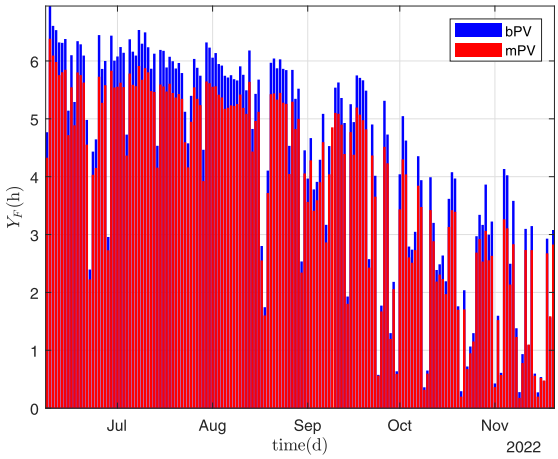

Fig. 4. Daily final yield Y_F of mPV (red) and bPV (blue).

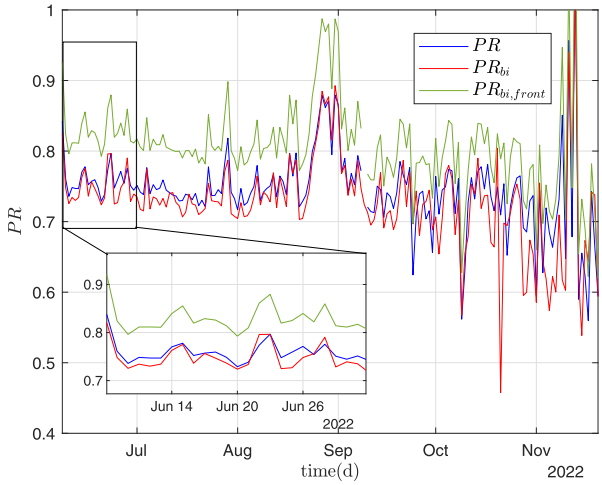

Fig. 5. Comparison among performance ratio PR, $\mathrm{PR_{bi}}$, and $\mathrm{PR_{bi,front}}$ formulas with focus on June.

many sunny days; during these days, the energy available on the front side of bPV modules, and mPV modules, is much higher than the energy per unit area available on the rear side of the bPV module. Given that the conversion efficiency of the front side is higher than the rear side, under these operating conditions, most of the energy generated by bPV modules is due to the irradiance on the front side. On the contrary, autumn months include a significant number of cloudy days, in which the difference between the energy available on the front and the rear side is less pronounced than on sunny days, mainly due to the strong reduction of direct irradiance. Under these operating conditions, the contribution of the rear side of a bPV module to the whole energy generated by the module itself becomes more significant.

In terms of the relative difference between mPV and bPV, the scientific literature showed contradictory results. For example, in [9], the highest relative difference of around 17.5% highlighted was detected in June and December. Instead, in a study developed in a snowy environment, the authors in [29] concluded that there is no significant difference between the bPV system and the mPV system in terms of energy yield; this difference is only evident during February when severe winter conditions predominate. According to a similar study conducted in Chengdu in China [30], bPV wall systems increase power generation by 19% in summer and 16% in winter compared with mPV systems. Therefore, the relative difference strongly depends on the climate and weather conditions, as well as the reflectivity of the ground behind the bPV modules, the height of the modules above the ground, and the angle of the modules relative to the sun.

A more detailed analysis of the energy generated can be performed on the basis of PR, that is computed according to (5) for the mPV system and (8) for the bPV system. The effect of temperature can be investigated by applying definitions (6) and (9). The contribution to the power conversion of the bPV module rear side can be investigated by applying the definition (5) on purpose to the bPV, although, according to the standard, this definition is specific to the mPV.

Fig. 5 shows the comparison of different daily PR formulas between mPV and bPV, and Table IV summarizes the PR for each analyzed month and over the whole testing period, as well as the final yield. The comparison among PR and $\mathrm{PR_{bi}}$ shows slightly better performance of bPV against mPV, especially during autumn months. Over the whole period, the results shows a better performance of bPV with an average PR of 1.76% higher

TABLE IV
PERFORMANCE RATIO COMPARISON

	PR mPV	PR_{bi} bPV	$PR_{bi,\,\mathrm{front}}$ bPV	$PR'_{25°C}$ mPV	$PR'_{25°C,bi}$ bPV
June⋆	0.7466	0.7577	0.8261	0.8432	0.8364
July	0.7284	0.7441	0.8075	0.8338	0.8313
August	0.7564	0.7674	0.8352	0.8539	0.8478
September	0.7304	0.7464	0.8025	0.7997	0.8025
October	0.7010	0.7381	0.7891	0.74	0.7689
November⋆⋆	0.6826	0.7197	0.7676	0.6869	0.7188
Whole Period	0.7325	0.7501	0.8117	0.8152	0.8176

⋆ From 8^{th} June. ⋆⋆ Until 20^{th} November.

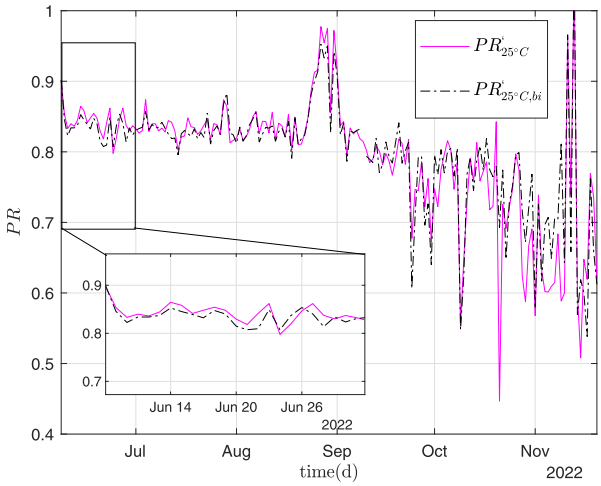

Fig. 6. Comparison among performance ratio $\mathrm{PR}'_{25°\mathrm{C}}$ and $\mathrm{PR}'_{25°\mathrm{C,bi}}$ formulas with focus on June.

than those of mPV. The whole period PR is 73.25% for mPV and 75.01% for bPV.

The comparison among $\mathrm{PR}'_{25°\mathrm{C}}$ and $\mathrm{PR}'_{25°\mathrm{C,bi}}$, which is shown in Fig. 6, highlights the effects of temperature on the power production. During summer months, they are quite similar. The difference between PR and $\mathrm{PR}'_{25°\mathrm{C}}$ is higher than the difference between $\mathrm{PR_{bi}}$ and $\mathrm{PR}'_{25°\mathrm{C,bi}}$ putting in evidence that bPV modules are characterized by lower temperature losses than mPV modules operating at the same high irradiance and high ambient temperature conditions.

Besides, in Fig. 7, two meaningful days, namely 16 October and 10 June, 2022, are shown where the recorded cell temperature of mPV (in red) and bPV (in blue) is depicted. In general, mPV cell temperature is higher than the bPV module; the recorded difference is proportional to the solar irradiance and the maximum value, corresponding to the higher solar irradiance close to 1000 $\mathrm{W/m^2}$, is nearly 5°C. This result is in agreement with the rated nominal operating cell temperature (NOCT) of the bPV and mPV modules: a temperature difference of nearly 4 °C is expected when the solar irradiance is 800 $\mathrm{W/m^2}$. The difference in the cell temperature is reasonably the cause of the difference between PR and $\mathrm{PR_{bi}}$, which is in the range of about $1\% - 1.5\%$, as given in Table IV, during summer months.

During autumn months, $\mathrm{PR}'_{25°\mathrm{C,bi}}$ is higher than $\mathrm{PR}'_{25°\mathrm{C}}$, the difference between PR and $\mathrm{PR}'_{25°\mathrm{C}}$ is quite similar to the difference between $\mathrm{PR_{bi}}$ and $\mathrm{PR}'_{25°\mathrm{C,bi}}$, showing again a little better performance of bPV against mPV. $\mathrm{PR_{bi,front}}$ is the PR computed for bPV modules by applying the definition proper of mPV (5),

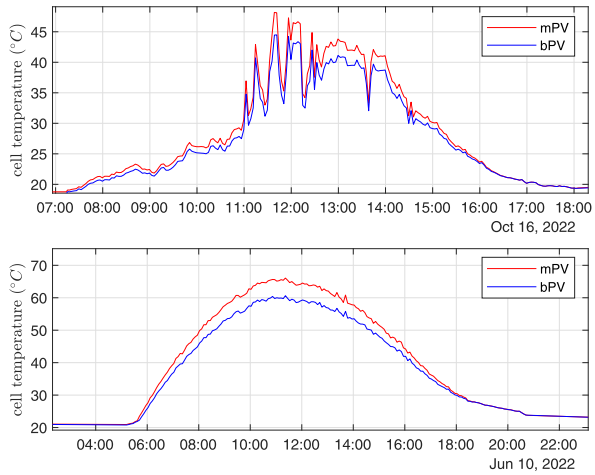

Fig. 7. Comparison between the cell temperatures of the mPV (in red) and bPV (in blue) in two meaningful days: 16 October and 10 June, 2022.

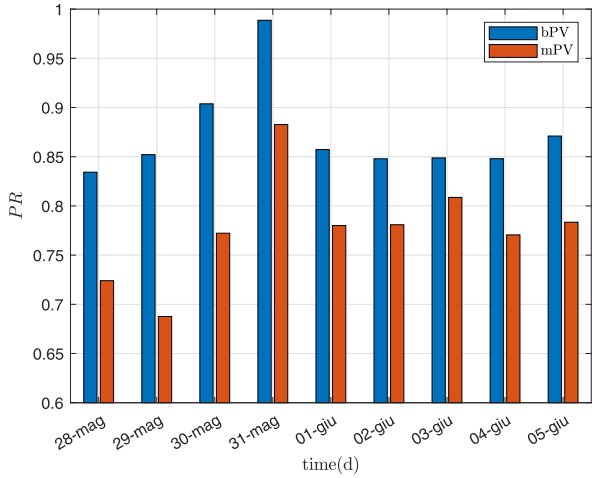

Fig. 8. Daily PR comparison between the mPV module and bPV module with the commercial white plastic sheet.

that do not take into account the irradiance on the rear side in the computation of Y_R. The comparison among PR and $\mathrm{PR_{bi,front}}$ highlights the contribution of the rear side of bPV modules to the power conversion. In the same installation and environmental conditions, the relative gain of the bPV technology compared with the mPV one is equal to 10.8%.

Fig. 8 shows the results, in terms of PR and $\mathrm{PR_{bi,front}}$ on a daily basis comparison for the configuration designed to enhance the effect of albedo on bPV. Over the 9-day testing period, the PR of the system based on mPV modules is 77.2% and the $\mathrm{PR_{bi,front}}$ of the system based on bPV modules is 86.8%, with a difference of 0.096. Compared with the monthly PRs of June (as highlighted in the focus of Fig. 5), the difference between PR and $\mathrm{PR_{bi,front}}$ is 0.0795, meaning that the enhancement of the albedo leads to an additional increase in the $\mathrm{PR_{bi,front}}$ of 0.0165, corresponding to a relative difference that increased of 20%.

V. CONCLUSION

This experimental research work assesses the enhanced performance of a bPV module in comparison with a traditional mPV module from 28 May to 20 November, 2022, in Milan. For this

purpose, some standard performance metrics were calculated and analyzed for both PV technologies with the aim to quantify the increase in the bPV energy performance.

The first experimental campaign, related to the comparison between the bPV modules and the mPV modules, highlighted that power output per unit and the final yield of the bPV module is higher than the one of mPV in every scenario. It was found that the PR relative gain of the bPV compared to mPV module is 10.8% higher in the whole period, demonstrating that the choice of implementing bPV technology is suggested instead of mPV from an energy yield point of view.

The second experimental campaign, related to the comparison between the bPV modules with a commercial white plastic sheet (adopted to increase the albedo) and the mPV modules, showed a PR with a similar trend but reveals that the bPV effectiveness suffers when the weather is particularly bad, even lower than the mPV counterpart. Overall, an improvement in the PR of an additional 0.0165 was obtained.

The study is carried out for a long period (i.e., six months) characterized by a high weather variability. However, the time span is still limited with respect to the operational lifetime of PV plants; therefore, further testing is needed.

In addition, the present work demonstrated that results cannot be generalized and results are very site specific.

Finally, future experimental activities should be addressed to assess the effect of: ground albedo using a more reflective surface, the elevation of bPV array, and the tilt angle variation on bPV power production. The combined action of all these factors can be studied to estimate the increase in the bifacial gain with respect to the base case presented in this study.

ACKNOWLEDGMENT

This manuscript reflects only the authors' views and opinions, neither the European Union nor the European Commission can be considered responsible for them.

REFERENCES

[1] A. Detollenaere et al., "Snapshot of global PV markets 2021 task 1 strategic PV analysis and outreach," Int. Energy Agency (IEV PVPS), Paris, France, Tech. Rep. IEA-PVPS T1-39, 2021.

[2] A. Metz, M. Fischer, and J. Trube, "International technology roadmap for photovoltaics (ITRPV): Crystalline silicon technology-current status and outlook," in *Proc. PV Manuf. Europe Conf.*, Brussels, Belgium, 2017, pp. 18–19.

[3] C. D. Rodríguez-Gallegos et al., "Monofacial vs bifacial Si-based PV modules: Which one is more cost-effective?," *Sol. Energy*, vol. 176, pp. 412–438, 2018.

[4] *Photovoltaic Devices - Part 1-2: Measurement of Current-Voltage Characteristics of Bifacial Photovoltaic (PV) Devices*, IEC Standard 60904-1-2:2019, IEC, Geneva, Switzerland, 2019. [Online]. Available: https://webstore.iec.ch/publication/34357

[5] M. Lamers et al., "Temperature effects of bifacial modules: Hotter or cooler?," *Sol. Energy Mater. Sol. Cells*, vol. 185, pp. 192–197, 2018.

[6] T. Liu et al., "Bifacial PV module operating temperature: High or low? A cross-comparison of thermal modeling results with outdoor on-site measurements," in *Proc. IEEE 48th Photovolt. Specialists Conf.*, 2021, pp. 2070–2073.

[7] *Photovoltaic (PV) Module Performance Testing and Energy Rating - Part 2: Spectral Responsivity, Incidence Angle and Module Operating Temperature Measurements*," IEC Standard IEC 61853-2, IEC, Geneva, Switzerland, 2016.

[8] G. Raina, R. Vijay, and S. Sinha, "Study on the optimum orientation of bifacial photovoltaic module," *Int. J. Energy Res.*, vol. 46, no. 4, pp. 4247–4266, 2022.

[9] W. Gu et al., "Experimental investigation of the bifacial photovoltaic module under real conditions," *Renewable Energy*, vol. 173, pp. 1111–1122, 2021.

[10] E. Molin, B. Stridh, A. Molin, and E. Wäckelgård, "Experimental yield study of bifacial PV modules in nordic conditions," *IEEE J. Photovolt.*, vol. 8, no. 6, pp. 1457–1463, Nov. 2018.

[11] W. Gu, T. Ma, S. Ahmed, Y. Zhang, and J. Peng, "A comprehensive review and outlook of bifacial photovoltaic (bPV) technology," *Energy Convers. Manage.*, vol. 223, 2020, Art. no. 113283.

[12] A. Asgharzadeh et al., "A sensitivity study of the impact of installation parameters and system configuration on the performance of bifacial PV arrays," *IEEE J. Photovolt.*, vol. 8, no. 3, pp. 798–805, May 2018.

[13] A. Asgharzadeh et al., "Analysis of the impact of installation parameters and system size on bifacial gain and energy yield of PV systems," in *Proc. IEEE 44th Photovolt. Specialist Conf.*, 2017, pp. 3333–3338.

[14] S. Wang et al., "Bifacial photovoltaic systems energy yield modelling," *Energy Procedia*, vol. 77, pp. 428–433, 2015.

[15] *Test Method for Reporting Photovoltaic Non-Concentrator System Performance*, Standard ASTM-E2848-13, 2013.

[16] *Photovoltaic System Performance–Part 2: Capacity Evaluation Method*, Standard IEC 61724-2:2016, IEC, Geneva, Switzerland, 2016. [Online]. Available: https://webstore.iec.ch/publication/25982

[17] M. Waters, C. Deline, J. Kemnitz, and J. Webber, "Suggested modifications for bifacial capacity testing," in *Proc. IEEE 46th Photovolt. Specialists Conf.*, 2019, pp. 1–6.

[18] K. Anderson, J. Kemnitz, and M. Boyd, "Evaluating cell temperature models and the effect of wind speed in PV system capacity testing," in *Proc. IEEE 48th Photovolt. Specialists Conf.*, 2021, pp. 1663–1669.

[19] K. S. Hayibo, A. Petsiuk, P. Mayville, L. Brown, and J. M. Pearce, "Monofacial vs bifacial solar photovoltaic systems in snowy environments," *Renewable Energy*, vol. 193, pp. 657–668, 2022.

[20] S. Hwang, H. S. Lee, and Y. Kang, "Energy yield comparison between monofacial photovoltaic modules with monofacial and bifacial cells in a carport," *Energy Rep.*, vol. 9, pp. 3148–3153, 2023.

[21] Solar Tech Lab. Accessed: Jun. 15, 2023. [Online]. Available: http://www.solartech.polimi.it

[22] *Photovoltaic System Performance–Part 1: Monitoring*, IEC Standard IEC 61724-1:2021, IEC, Geneva, Switzerland, 2021. [Online]. Available: https://webstore.iec.ch/publication/65561

[23] S. Leva, M. Mussetta, and E. Ogliari, "PV module fault diagnosis based on microconverters and day-ahead forecast," *IEEE Trans. Ind. Electron.*, vol. 66, no. 5, pp. 3928–3937, May 2019.

[24] A. Dolara, S. Leva, G. Manzolini, and E. Ogliari, "Investigation on performance decay on photovoltaic modules: Snail trails and cell microcracks," *IEEE J. Photovolt.*, vol. 4, no. 5, pp. 1204–1211, Sep. 2014.

[25] N. Matera, D. Mazzeo, C. Baglivo, and P. M. Congedo, "Will climate change affect photovoltaic performances? A long-term analysis from 1971 to 2100 in Italy," *Energies*, vol. 15, no. 24, 2022, Art. no. 9546.

[26] *Photovoltaic Devices - Part 1: Measurement of Photovoltaic Current-Voltage Characteristics*, IEC Standard IEC 60904-1:2020, IEC, Geneva, Switzerland, 2020. [Online]. Available: https://webstore.iec.ch/publication/32004

[27] A. Dolara et al., "Outdoor assessment and performance evaluation of OPV modules," *IEEE J. Photovolt.*, vol. 11, no. 2, pp. 391–399, Mar. 2021.

[28] J. A. Duffie and W. A. Beckman, "Available solar radiation," in *Solar Engineering of Thermal Processes*. Hoboken, NJ, USA: Wiley, 2013, ch. 2, pp. 43–137. [Online]. Available: https://onlinelibrary.wiley.com/doi/abs/10.1002/9781118671603.ch2

[29] K. S. Hayibo, A. Petsiuk, P. Mayville, L. Brown, and J. M. Pearce, "Monofacial vs bifacial solar photovoltaic systems in snowy environments," *Renewable Energy*, vol. 193, pp. 657–668, 2022.

[30] O. Zhao et al., "Experimental and numerical study on the performance of innovative bifacial photovoltaic wall system," *Sustain. Cities Soc.*, vol. 85, 2022, Art. no. 104085.

Open Access funding provided by 'Politecnico di Milano' within the CRUI CARE Agreement